Nuclear Magnetic Resonance Investigations of Configurational Non-rigidity in Dinuclear Platinum(IV) Complexes. Part 7.† Intramolecular Rearrangements in Complexes of Tris(methylthio)methane

Edward W. Abel, Thomas E. MacKenzie, Keith G. Orrell,* and Vladimir Sik
Department of Chemistry, University of Exeter, Exeter EX4 4QD

The ligand tris(methylthio)methane, $HC(SMe)_3$, has been used to form dinuclear platinum(IV) complexes of type $[(PtXMe_3)_2\{HC(SMe)_3\}]$ (X = Cl or Br), where the ligand bridges the pair of Pt atoms *via* two of its SMe groups. Variable-temperature ^1H n.m.r. studies in the range −90 to 70 °C revealed inversion of the pyramidal S atoms, a 1,3-metal pivoting fluxion, and a scrambling of the Pt-methyl environments by a $PtMe_3$ rotation mechanism. The latter two fluxions are concerted and involve a common transition state. Activation energies for the various dynamic processes are in the range 45—72 kJ mol^{-1}.

The stereodynamics of dinuclear platinum(IV) complexes of type $[(PtXMe_3)_2L]$ (X = halogen) have been explored in previous studies in this series. Such dinuclear complexes are formed with ease using acyclic or cyclic ligands (L), when there is no more than one carbon atom between potential donor sites. Thus, previous studies have been concerned with complexes with L = $MeECH_2EMe$,[1] MeEEMe (E = S or Se),[2] $SCH_2SCH_2SCH_2$,[3] $SCH_2SCH_2SCH_2SCH_2$,[4] $MeSCH_2SeMe$,[5] and $ECH_2CMe_2CH_2E$ (E = S or Se).[6] However, the tris(methylthio)methane molecule, $HC(SMe)_3$, also satisfies the above criterion and the present work was undertaken to synthesize and to examine the structural dynamics of its platinum(IV) complexes using dynamic nuclear magnetic resonance (d.n.m.r.) methods. The latter have been particularly valuable previously in revealing low-temperature pyramidal inversions of co-ordinated chalcogen atoms, ligand fluxions involving 60, 90, or 180° rotations of the ligand relative to the $(PtXMe_3)_2$ moiety, and platinum methyl scramblings. Particular interest in the present complexes centres round the nature of the $HC(SMe)_3$ ligand fluxions and their direct or indirect involvement with any platinum methyl scramblings.

Experimental

Materials. The ligand $HC(SMe)_3$ was prepared by a literature method.[7] Trimethylplatinum(IV) halide complexes of this ligand were prepared by direct action with $[(PtXMe_3)_4]$ in the appropriate solvent. Full details for the chloro complex are given as an example.

Di-μ-chloro-μ-tris(methylthio)methane-bis[trimethylplatinum(IV)].—Tris(methylthio)methane (54 mg, 0.36 mmol) and trimethylplatinum(IV) chloride (198 mg, 0.73 mmol)+ were dissolved in chloroform (7 cm^3) in a Schlenk tube. The solution was refluxed for 24 h after which the solvent was removed giving an off-white powder. This was crystallized from chloroform–hexane to give colourless crystals (207 mg, 79%), m.p. 173 °C (Found: C, 17.05; H, 4.00. Calc. for $C_{10}H_{27}Cl_2Pt_2S_3$: C, 16.95; H, 3.95%).

Di-μ-bromo-μ-tris(methylthio)methane-bis[trimethylplatinum(IV)]. This was prepared by the same method as for the chloro complex, except that dichloromethane was used as solvent, giving colourless crystals, m.p. 165 °C (Found: C, 15.1; H, 3.55. Calc. for $C_{10}H_{27}Br_2Pt_2S_3$: C, 14.9; H, 3.65%).

The dinuclear complex $[(PtIMe_3)_2\{HC(SMe)_3\}]$ could not be isolated in the pure state. Prolonged heating (*ca.* 48 h) of $[(PtIMe_3)_4]$ with $HC(SMe)_3$ in a Carius tube containing heptane yielded a small amount of an off-white crystalline solid in addition to black platinum residues. The 400-MHz ^1H n.m.r. spectrum of the white solid (in CD_2Cl_2) consisted of two interpenetrating quintets [$^3J(PtH) \sim 16$ Hz] in the intensity ratio 2:1, indicating two types of bridging thiomethyl groups. In the Pt-methyl region three distinct signals, each with ^{195}Pt satellites, were observed in the intensity ratio 1:2:1. Two of the $^2J(PtH)$ couplings imply environments *trans* to I, while the third coupling is consistent with PtMe *trans* to S.[8] These data are clearly incompatible with a simple dinuclear complex $[(PtIMe_3)_2L]$, but the limited amount of material isolated prevented further investigations into its structure.

N.M.R. Studies.—Most ^1H spectra were measured using a JEOL PS/PFT-100 spectrometer operating at 100 MHz. A JES-VT-3 accessory was used to control the probe temperature within the range −90 to 105 °C. Temperatures were measured to within 1 °C using a Comark digital thermometer (Type 5000) attached to a Cu/Cu–Ni thermocouple. The complexes were dissolved in either CD_2Cl_2 or $CDCl_3$ depending on the temperature. In one or two instances where greater chemical shift dispersion was required, 400-MHz ^1H spectra were obtained by courtesy of the S.E.R.C. n.m.r. service at Warwick University.

Total n.m.r. bandshape analyses were performed with our version of the DNMR3 program of Kleier and Binsch.[9] Rate constants were based on the optimal visual fits of experimental and computer synthesized spectra. Errors quoted for $\Delta G^{\ddagger}$ data follow previous work.[10]

Results

Unlike other dinuclear complexes in this series, two possible configurational isomers may occur with the ligand $HC(SMe)_3$, depending on whether the methine proton or the unco-ordinated thiomethyl group occupies the apical bridge position in the complex. An inspection of the low-temperature (−90 °C) ^1H spectrum of complex $[(PtClMe_3)_2\{HC(SMe)_3\}]$ reveals two methine signals as 1:8:18:8:1 quintets due to equivalent coupling to two Pt atoms. The intensity ratio of these quintets

† Part 6 is ref. 6.

+ Molar quantities are based on the monomeric unit $PtClMe_3$.

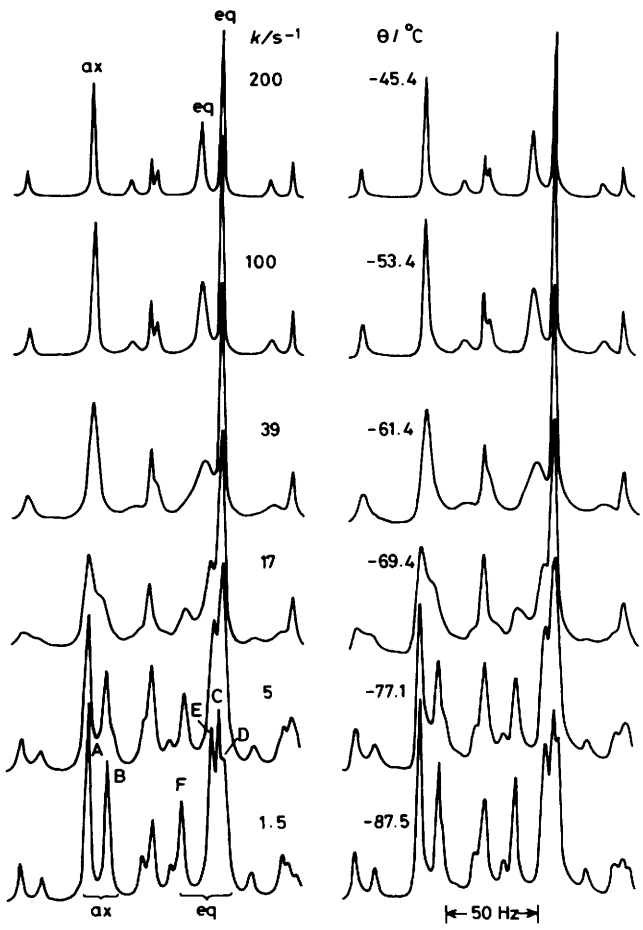

Figure 1. 100-MHz ^{1}H n.m.r. spectra of the Pt-methyl region of $[(PtClMe_3)_2\{HC(SMe)_3\}]$. Experimental spectra on the right, 'best-fit' computer synthesized spectra on the left. Signal labelling refers to Figure 3

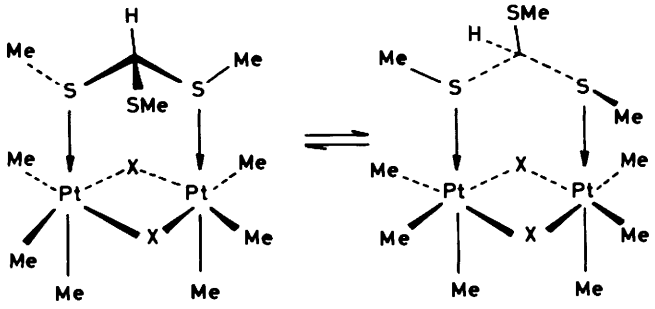

Figure 2. The effects of reversal of the -SCH(SMe)S- portion of the six-membered ring on the DL invertomer of $[(PtXMe_3)_2\{HC(SMe)_3\}]$

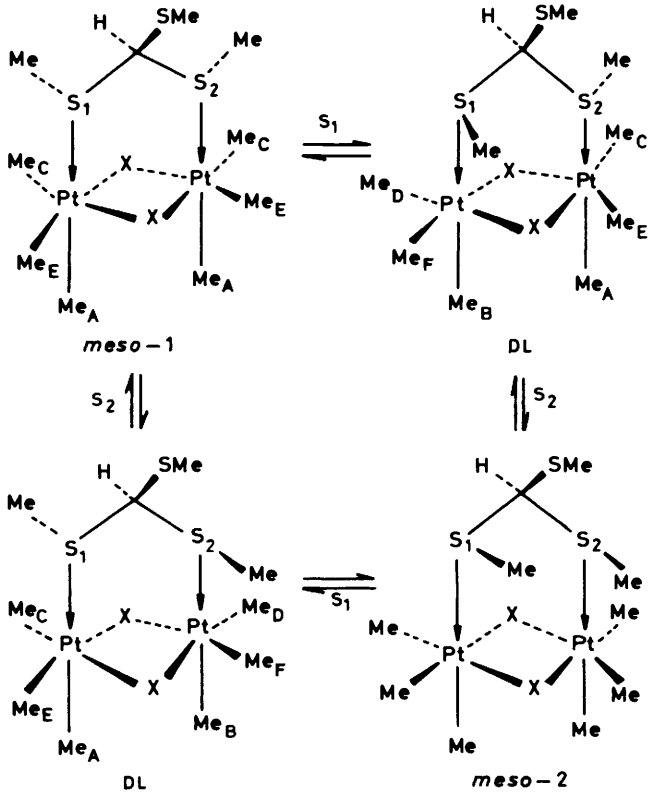

Figure 3. The effects of sulphur inversion in the complexes $[(PtXMe_3)_2\{HC(SMe)_3\}]$. The *meso*-2 form was undetected

is *ca.* 82:18. The platinum methyl region of the spectrum comprises six signals each with ^{195}Pt satellites (Figure 1). The two signals at highest frequency have ^2J(PtH) values of *ca.* 70 Hz indicating methyls *trans* to sulphur (*i.e.* axial) while the other four signals have values around 77 Hz due to methyls *trans* to a bridging halogen (*i.e.* equatorial).[8] The ligand methyl region of the spectrum is rather unclear. Two 1:4:1 triplets due to co-ordinated SMe groups are detectable together with a singlet due to a bridging SMe group. In addition, other weaker overlapping signals are also present, rendering a full analysis uncertain.

At this low temperature (−87.5 °C) the pyramidal inversion of the two sulphur atoms will be slow and each configurational isomer can give rise to three n.m.r.-distinguishable invertomers, namely *meso*-1, *meso*-2, and a degenerate DL pair.[1] If all six n.m.r.-distinguishable invertomers are present then six CH signals, and as many as 24 PtMe signals, are possible. The presence of only two CH signals and six PtMe signals clearly indicates far fewer detectable species than are theoretically possible. The ^3J(PtH) couplings associated with both CH signals have a magnitude of 5.6 Hz at −87.5 °C, and these are of considerable diagnostic importance. When the methine proton is in the apical position, then the dihedral angle of the fragment Pt–S–C–H is *ca.* 180°, compared to *ca.* 60° if the methine were non-apical. According to the Karplus theory,[11] greater ^3J(PtH) coupling is expected in the former case. This argument was used to assign the ring methylene protons in the 1,3,5-trithiane and 1,3,5,7-tetrathiocane complexes $[(PtXMe_3)_2\{(SCH_2)_n\}]$ (n = 3[3] or 4[5]). In these cases the ^3J(PtH) values for the bridging methylene protons had magnitudes of 14—15 Hz and *ca.* 1 Hz, the larger values being associated with the axial ring protons. In the present complexes the ^3J(PtH) values of 5.6 Hz strongly suggest a Pt–S–C–H dihedral angle closer to 60 than 180°. Such a situation can be achieved by assuming a rapid reversal of the -SCH(SMe)S- portion of the six-membered ring formed between the ligand and the dinuclear Pt moiety (Figure 2). Strong support for such a suggestion comes from earlier work[1] on the complexes $[(PtXMe_3)_2(MeSCH_2SMe)]$ where actual barrier energies for this type of ring reversal process were measured. Whereas in the previous complexes the ring reversal rates affected the ^{1}H spectra at temperatures below *ca.* −70 °C, in the present complexes no such effects were found, and it must be concluded that the process is still rapid on the n.m.r. time-scale at −87.5 °C, the lowest temperature reached.

Table 1. Ligand proton n.m.r. parameters[a] for $[(PtXMe_3)_2\{HC(SMe)_3\}]$ complexes

		Methine				S–Me					
X	θ/°C	δ_1	δ_2	$^3J(PtH_1)$	$^3J(PtH_2)$	δ_1	δ_2	δ_3	$^3J(PtH_1)$	$^3J(PtH_2)$	$^3J(PtH_3)$
Cl[b]	−90	5.71	5.83	5.6	5.6	2.68	2.44	2.41	11.6	13.2	~0
	25.7	5.65		3.0		2.54		2.37	11.8		~0
Br[c]	−90	5.79	~5.85	5.6	5.6	2.71	2.43	2.43	12.1	13.9	~0
	−26.3	5.72		3.4		2.55		2.38	12.7		~0

[a] All chemical shift values in p.p.m. relative to $SiMe_4$; J values in Hz. [b] DL 81.8%, *meso*-1 18.2%. [c] DL 88.7%, *meso*-1 11.3%.

Table 2. Pt-methyl ^1H n.m.r. parameters* for $[(PtXMe_3)_2\{HC(SMe)_3\}]$ complexes

		Axial Pt–Me				Equatorial Pt–Me							
X	θ/°C	δ_A	δ_B	$^2J(PtH_A)$	$^3J(PtH_B)$	δ_F	δ_E	δ_C	δ_D	$^2J(PtH_F)$	$^2J(PtH_E)$	$^2J(PtH_C)$	$^2J(PtH_D)$
Cl	−87.5	1.57	1.46	70.9	70.3	1.05	0.89	0.85	0.81	77.3	76.4	75.2	78.7
	25.7	1.65		71.6		0.98		0.87		76.6		76.9	
Br	−87.5	1.69	1.60	71.4	71.0	1.12	0.97	0.92	0.89	75.9	75.6	75.2	77.2
	−26.3	1.76		71.3		1.07		0.95		75.4		75.4	

* All chemical shifts in p.p.m. relative to $SiMe_4$; J values in Hz.

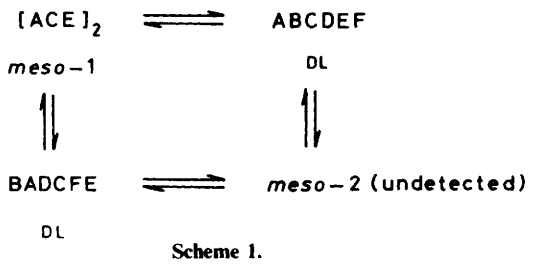

Scheme 1.

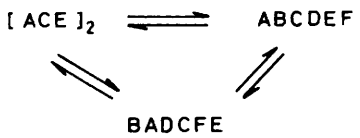

Scheme 2.

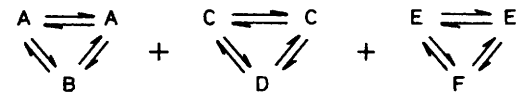

Scheme 3.

Scheme 4.

The low-temperature n.m.r. spectra are therefore due to the effects of slow sulphur inversion on the single time-averaged configurational isomer of the complexes. The observed pair of CH signals may therefore be attributed to two of three n.m.r.-distinguishable invertomers shown in Figure 3. Previous experience of these types of system strongly suggests that the most abundant invertomer will be DL, probably followed by *meso*-1. Such a mixture should give rise to nine PtMe signals (six signals for DL and three for *meso*-1). However, the environments of the three Pt-methyls in the *meso*-1 invertomer will closely match those of *one* of the two distinct $PtMe_3$ moieties of the DL invertomer. Virtually identical chemical shifts are therefore very likely, thus explaining the observed total of six PtMe signals. These signals separate into two axial and four equatorial Pt-methyls. Chemical shift and spin coupling constant data for both the chloro and bromo complexes are given in Tables 1 and 2.

Sulphur Inversion.—On raising the temperature of the complexes to *ca.* −40 °C, the spectra change in the way illustrated in Figure 1 for the chloro complex, namely the two axial PtMe signals coalesce and sharpen to a singlet (with satellites), and the four equatorial PtMe signals coalesce to two signals (with satellites). Clearly this is the result of pyramidal inversions of the sulphur atoms becoming fast in relation to the n.m.r. detection time-scale. In order to perform bandshape fittings on these spectra it is necessary to know which of the three pairs of signals at low temperature subsequently undergo mutual exchange as a result of the inversion process. The dynamic spin problem for the Pt-methyls is as in Scheme 1, which is equivalent to Scheme 2, where the labelling using the notation of Haigh[12] refers to Figure 3. Since no methyl–methyl couplings were detected, the spin problem can be split into subsets, Scheme 3, which is equivalent to Scheme 4, where the invertomer populations (p) are given below.

$$p_A = p_C = p_E = p(meso\text{-}1) + \tfrac{1}{2}p(DL)$$
$$p_B = p_D = p_F = \tfrac{1}{2}p(DL)$$

The assignments of the six PtMe signals to methyls Me_A—Me_F are given in Table 2. Most of these assignments are unambiguous. Thus, chemical shift and relative intensity considerations attribute the two highest frequency signals to the two axial PtMe groups. The signal at δ 1.05 clearly exchanges with one of the group of three lowest frequency signals. A careful inspection of the bandshape changes shows the exchange is with the signal at δ 0.89. This was subsequently confirmed by the computer fittings. The remaining closely separated pair of signals at δ 0.85 and 0.81 must therefore mutually exchange but with little line broadening. Using the chemical shift and coupling constant data in Table 2, the Pt-methyl spectra were fitted using the DNMR3 program.[9] The ^{195}Pt satellites were

Table 3. Energy parameters for sulphur inversion in $[(PtXMe_3)_2\{HC(SMe)_3\}]$ complexes

X	E_a/kJ mol^{-1}	$\log_{10}(A/s^{-1})$	$\Delta G^{\ddagger}$* kJ mol^{-1}	$\Delta H^{\ddagger}$ kJ mol^{-1}	$\Delta S^{\ddagger}$ J K^{-1} mol^{-1}
Cl	44.6	12.6	45.5	42.9	−8.6
Br	45.0	12.8	45.0	43.3	−5.8

* Measured at 298.15 K; maximum error ±1.3 kJ mol^{-1}.

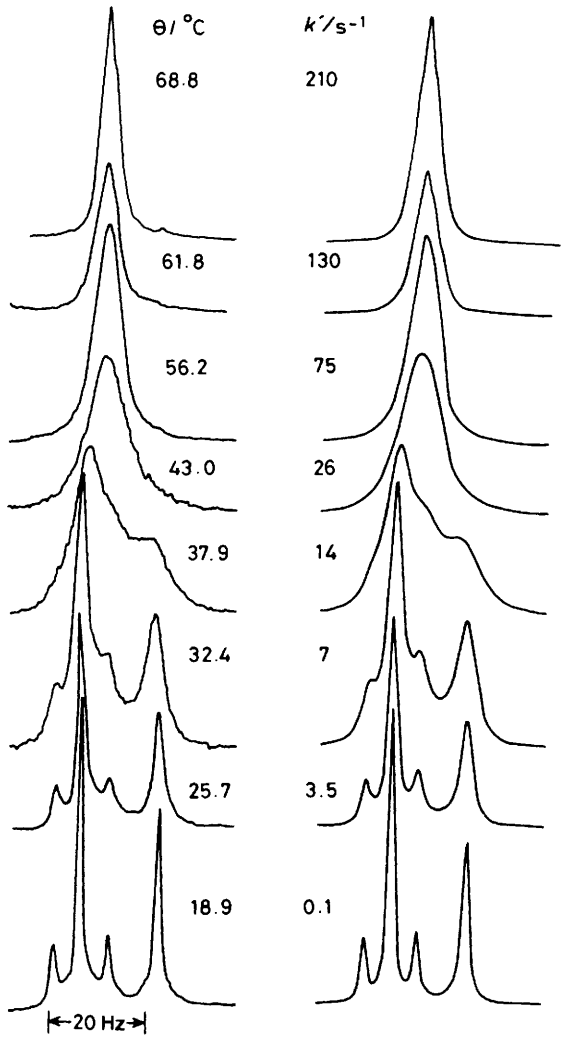

Figure 4. The high-temperature 100-MHz ^{1}H spectra of $[(PtClMe_3)_2\{HC(SMe)_3\}]$ showing the effects of 1,3-ligand pivoting on the S-methyl signals (experimental on left, computer synthesized spectra on right)

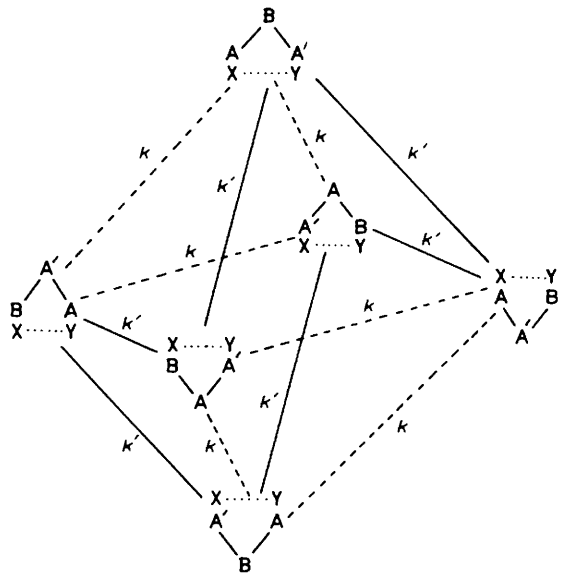

Figure 5. Graph diagram depicting the possible fluxional mechanisms in $[(PtXMe_3)_2\{HC(SMe)_3\}]$: (——) 60° pivot, ( ) 120° rotation

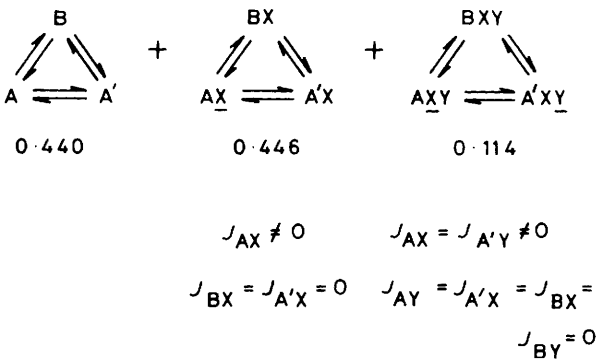

Scheme 5.

also taken into account and the optimum fitted spectra are shown alongside the experimental spectra in Figure 1. Arrhenius and Eyring parameters were calculated in the usual way and the results are collected in Table 3.

Fluxional Processes.— On further heating the complexes in solution, additional n.m.r. bandshape changes were observed, particularly in the temperature range 20—70 °C. In this range the SMe region of the spectrum is informative, with the co-ordinated and unco-ordinated SMe signals coalescing to a singlet at *ca.* 70 °C (Figure 4). Gross changes also take place in the PtMe region of the spectrum, leading to loss of distinction between axial and equatorial methyls (see later). The retention of ^{195}Pt coupling of the PtMe signals and the semblance of ^{195}Pt satellites in the high-temperature averaged SMe signal point to the fluxional process(es) being intramolecular. The poorly resolved nature of SMe satellites is not surprising as the high-temperature averaged coupling to ^{195}Pt will be approximately one-third that of the low-temperature value. The resulting averaged J coupling of 3—4 Hz is only just greater than the measured spectral bandwidth at 70 °C. However, a somewhat better defined ^{195}Pt satellite structure of the CH signal strengthens the evidence for an intramolecular fluxion.

There are two possible explanations of the ligand methyl equilibration. The first is a synchronous 1,3-shifting of both Pt atoms, equivalent to a series of 120° rotations of the ligand relative to the dinuclear Pt moiety, while the second possible mechanism is a series of 60° pivots of the ligand about *either* of the Pt–S bonds. Representing the ligand methyls by the labels A, A′, and B, and the two Pt atoms by X and Y, the total

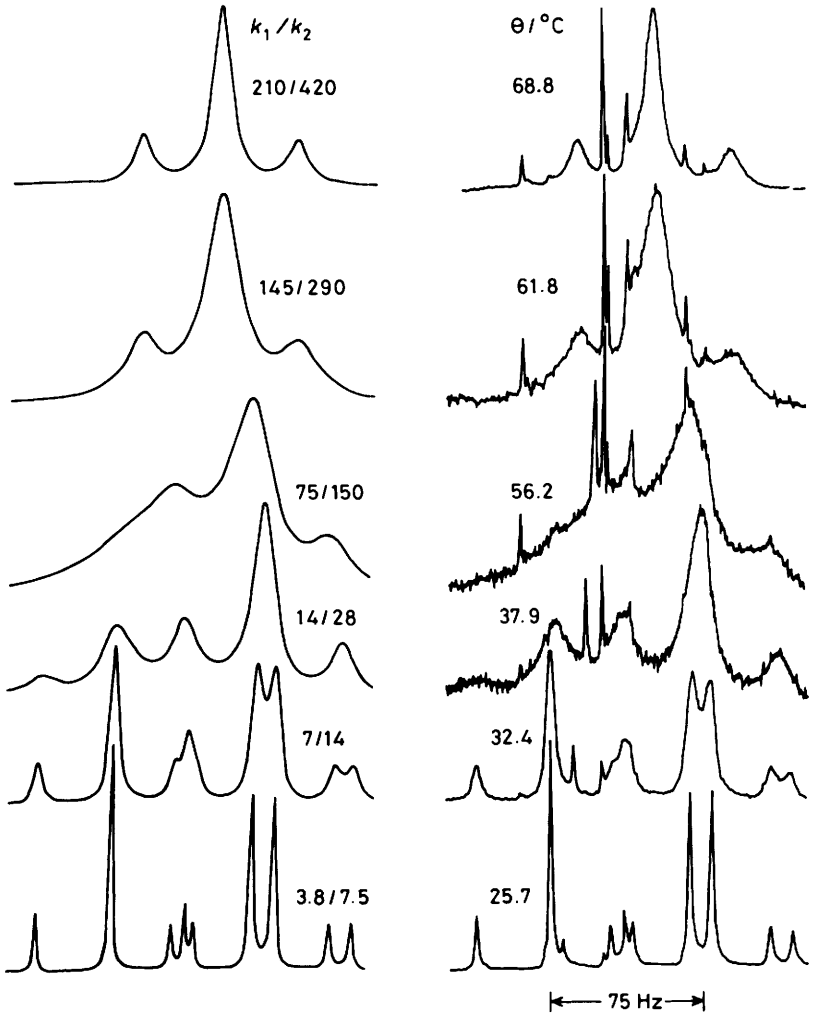

Figure 6. The high-temperature 100-MHz ^1H spectra of the Pt-methyl region of $[(PtClMe_3)_2\{HC(SMe)_3\}]$ showing the effects of the fluxional rearrangement; k_1 and k_2 are the best-fit rate constants for ax–eq and eq–eq exchange respectively (experimental on right, computer synthesized spectra on left)

configurational net resulting from these two mechanisms is shown in Figure 5. It should be noted that X and Y are purely labels and denote isochronous Pt atoms, whereas the labels A, A′, and B reflect the two different chemical shifts of the ligand methyls in the configurations forming the apex and base of the graph diagram (Figure 5). A careful study of Figure 5 shows that for either process, exchange between the A (or A′) and B methyl environments occurs at the same rate, either with a rotation rate constant k or a pivot rate constant k'. Even when the spin-active Pt species are taken into account the dynamic spin system for both mechanisms is identical, Scheme 5 (underlined labels refer to spin-active ^{195}Pt).

At first sight Scheme 5 might appear to be incorrect for the pivoting of the single ^{195}Pt species. Whereas three 120° rotations are required to restore ^{195}Pt coupling, five 60° pivots are required to restore this coupling. However, within the complete cycle of six pivots, *two* of the configurations retain ^{195}Pt–Me coupling and therefore the rate of restoration of Pt coupling is the same as for the rotation process, namely three single-step changes on average.

The experimental spectra in the approximate temperature range 15—70 °C were fitted according to the above dynamic system (Scheme 5) and excellent fits obtained. The results for the chloro complex are shown in Figure 4.

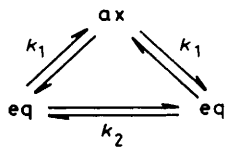

Scheme 6.

Distinction between the rotation and pivot mechanisms can be achieved, however, by a careful evaluation of the Pt-methyl region of the spectra (Figure 6). The bandshape changes in this region depend in a subtle way on the fluxional mechanism(s) operating. The important observation is that the ligand rotation mechanism will cause no equatorial PtMe averaging whereas the pivot process will. The high-temperature spectra clearly depict some type of movement between the three PtMe environments. If this methyl scrambling process is not correlated with the ligand fluxion, then the rate constants for ax–eq and eq–eq methyl exchanges, denoted by k_1 and k_2 respectively, should bear no relation to the ligand fluxion rate constant k or k'. In order to test this point, the PtMe region spectra were therefore fitted by allowing for free variation of the rate constants k_1 and k_2 according to Scheme 6.

The best-fit values for the chloro complex are shown in Figure

Table 4. Energy data for the ligand pivot/Pt-methyl scrambling fluxion in $[(PtXMe_3)_2\{HC(SMe)_3\}]$ complexes

X	Signals	E_a/kJ mol^{-1}	$\log_{10}(A/s^{-1})$	$\Delta G^{\ddagger}$*/kJ mol^{-1}	$\Delta H^{\ddagger}$/kJ mol^{-1}	$\Delta S^{\ddagger}$/J K^{-1} mol^{-1}
Cl	SMe	77.9 ± 0.5	13.9 ± 0.5	71.7 ± 0.2	75.0 ± 2.8	11.2 ± 8.9
Cl	PtMe	75.7 ± 0.9	13.5 ± 0.1	71.9 ± 0.1	73.2 ± 0.9	4.3 ± 2.8
Br	SMe	76.7 ± 2.1	14.1 ± 0.4	69.5 ± 0.1	74.2 ± 2.1	15.6 ± 6.6
Br	PtMe	76.8 ± 1.5	14.1 ± 0.3	69.4 ± 0.1	74.2 ± 1.5	16.0 ± 4.9

* Values at 298.15 K.

Table 5. Sulphur inversion energies in related $[(PtXMe_3)_2L]$ complexes

L	X	$\Delta G^{\ddagger}$[a]/kJ mol^{-1}	Ref.
$HC(SMe)_3$	Cl	45.5	*b*
$HC(SMe)_3$	Br	45.0	*b*
$MeSCH_2SMe$	Cl	48.5	1
$MeSCH_2SMe$	Br	44.6	1
MeSCHMeSMe	Cl	43.3	1
MeSCHMeSMe	Br	43.5	1
MeSSMe	Cl	41.4	2
MeSSMe	Br	40.7	2
$Me_2\overline{CCH_2SSCH_2}$	Cl	66.2	6,13
$Me_2\overline{CCH_2SSCH_2}$	Br	66.0	6,13

[a] All data at 298.15 K. [b] This work.

Table 6. Energy data for high-energy fluxions in $[(PtXMe_3)_2L]$ complexes

L	X	Process[a]	$\Delta G^{\ddagger}$[b]/kJ mol^{-1}	Ref.
$HC(SMe)_3$	Cl	LP	71.7	*c*
		MS	71.9	
$HC(SMe)_3$	Br	LP	69.5	*c*
		MS	69.4	
MeSCHMeSMe	Cl	LS	71.5	1
		MS	71.6	
MeSSMe	Cl	LS	61.3	2
		MS	62.4	
$Me_2\overline{CCH_2SSCH_2}$	Cl	MS	71.4	6
$Me_2\overline{CCH_2SSCH_2}$	Br	MS	71.2	6
$(\overline{SCH_2})_4$	Cl	LP	66.1	5
		MS	65.8	
$(\overline{SCH_2})_4$	Br	LP	63.9	5
		MS	64.0	
$(\overline{SCH_2})_3$	Cl	LP	58.6	3
		MS	71.1	
$(\overline{SCH_2})_3$	Br	LP	58.8	3
		MS	67.4	

[a] LP = ligand pivoting, LS = ligand switching, MS = methyl scrambling. [b] All data at 298.15 K. [c] This work.

6. These should then be compared with those in Figure 4. It will be apparent immediately that, for any given temperature, $k_2 \approx 2k_1$ and $k_1 \approx k'$. This implies that $k_2 \approx k' + k_1$. In other words, the spectra appear to show eq–eq methyl exchange arising from both the ligand fluxion and the Pt-methyl scrambling fluxion, proving that the former must occur by the 60° pivot mechanism. Furthermore, the ax–eq methyl exchange rate matches the ligand pivot rate at any temperature which strongly implies a single transition state for both fluxions. Energies for this methyl exchange process based on the Pt-methyl region spectra were computed using the usual Arrhenius and Eyring theories and the results given in Table 4.

Discussion

The sulphur inversion energies computed for the present complexes (Table 3) compare favourably with values obtained for related co-ordinated sulphur ligand complexes (Table 5). Values of the Gibbs free energy change $\Delta G^{\ddagger}$ for inversion in open-chain 1,3-chalcogen ligands lie in the narrow range 43—48 kJ mol^{-1}. There is little halogen dependence, as noted previously,[1] and clearly the ease of pyramidal inversion is governed by the nature of the Pt–S bonds. When these are more highly strained as in the dimethyl disulphide complexes $[(PtXMe_3)_2(MeSSMe)]$ then there is slightly easier access to the transition state structure for inversion and the energy barrier decreases somewhat.

In previous dinuclear Pt^{IV} complexes,[1,2] only the DL invertomer has been detected at low temperatures. The n.m.r. spectra therefore were sensitive only to double sulphur inversion leading to the production of the other DL invertomer. Whether or not this double inversion was a truly synchronous process or a correlated consecutive process was a moot point although the latter process was favoured on energetic grounds.[2] In the present complexes, although both DL and *meso*-1 species were detected, the *meso*-1 invertomer could not be separately distinguished from the DL invertomer by its Pt-methyl signals. Therefore, the PtMe spectral changes could be interpreted as being either *meso*-1 $\rightleftharpoons$ DL or DL $\rightleftharpoons$ DL exchanges. Totally unambiguous evidence for single-site inversion in these dinuclear Pt^{IV} complexes therefore still eludes us. It is, however, intuitively the more reasonable process, particularly now that it has been established recently that a synchronous process involving a substantially higher energy transition state will only occur when geometric constraints force it to be the only possible mechanism, as in the complexes $[(PtXMe_3)_2(Me_2\overline{CCH_2SSCH_2})]$.[6,13]

The Arrhenius and Eyring energy data for the high-temperature fluxion(s) in the present complexes are contained in Table 4. The Eyring parameters $\Delta G^{\ddagger}$ and $\Delta H^{\ddagger}$ for the ligand pivot process and the methyl scrambling process are identical within experimental error. Values of $\Delta G^{\ddagger}$ calculated for analogous fluxions in related complexes of type $[(PtXMe_3)_2L]$ are shown in Table 6. In the other cases where ligand pivoting is occurring, the $\Delta G^{\ddagger}$ values decrease with ligand in the sequence $HC(SMe)_3 > (\overline{SCH_2})_4 > (\overline{SCH_2})_3$. This suggests that the pivot process is favoured when the non-co-ordinated S atoms are constrained by the ligand ring to more favourable positions for achieving the pivot transition state. The very closely related complex $[(PtClMe_3)_2(MeSCHMeSMe)]$ possesses the most similar $\Delta G^{\ddagger}$ data despite the fact that the ligand in the latter complex is undergoing 180° switches rather than 60° pivots. In all cases except that of $[(PtXMe_3)_2\{(\overline{SCH_2})_3\}]$ (X = Cl or Br),[3] the energies for the fluxions calculated from the ligand methyl and the Pt-methyl regions of the spectra are equal within

experimental error, which strongly infers that a single concerted fluxion with a single seven-co-ordinate Pt^{IV} transition state is operating. This conclusion has already been reached following the detailed d.n.m.r. analysis of the spectra of $[(PtXMe_3)_2\{(\overset{\square}{S}CH_2)_4\}]$.[5] In that work, a model involving 60° ligand pivots together with 120° rotations of the pendant $PtMe_3$ moiety about its three-fold rotation axis completely explained the observed spectral changes, and in particular it provided a rationalization for the rate of Pt-methyl eq–eq exchange being twice that of ax–eq exchange. A similar relationship between the Pt-methyl exchanges was found in the present complexes and an almost exactly parallel argument to that given previously[5] can be applied.

The fluxionality of the $[(PtXMe_3)_2\{(\overset{\square}{S}CH_2)_3\}]$ complexes is rather akin to that of the present complexes, and indeed the graph diagram depicting the ligand pivot and rotation mechanisms in the present work (Figure 5) is analogous to that used for the 1,3,5-trithiane complexes (see Figure 6, ref. 3). However, the energy data for the latter complexes are anomalous in that they clearly show that Pt-methyl scrambling does not occur concurrently with the ligand 1,3-pivoting. The reason for this is unclear, but the implication is that in these 1,3,5-trithiane complexes the transition state associated with the 1,3-pivot process is insufficiently activated to induce exchange of Pt-methyl environments. From the $\Delta S^{\ddagger}$ data,[3] it would appear that the latter process only occurs as a consequence of ligand dissociation/recombination.

In conclusion, the dynamic stereochemistry of the $[(PtXMe_3)_2\{HC(SMe)_3\}]$ (X = Cl or Br) complexes can be described in terms of pyramidal inversions of co-ordinated S atoms, followed, at somewhat higher temperatures, by 1,3-pivoting of the $HC(SMe)_3$ ligand and concurrent 120° rotations of the pendant $PtMe_3$ moiety.

Acknowledgements

We wish to thank the S.E.R.C. for use of the high-field n.m.r. service at the University of Warwick for some of the ^1H n.m.r. spectra.

References

1 E. W. Abel, A. R. Khan, K. Kite, K. G. Orrell, and V. Sik, *J. Chem. Soc., Dalton Trans.*, 1980, 2208.
2 E. W. Abel, A. R. Khan, K. Kite, K. G. Orrell, and V. Sik, *J. Chem. Soc., Dalton Trans.*, 1980, 2220.
3 E. W. Abel, M. Booth, G. D. King, K. G. Orrell, G. M. Pring, and V. Šik, *J. Chem. Soc., Dalton Trans.*, 1981, 1846.
4 E. W. Abel, K. Kite, K. G. Orrell, V. Sik, and B. L. Williams, *J. Chem. Soc., Dalton Trans.*, 1981, 2439.
5 E. W. Abel, G. D. King, K. G. Orrell, V. Sik, T. S. Cameron, and K. Jochem, *J. Chem. Soc., Dalton Trans.*, 1984, 2047.
6 E. W. Abel, P. K. Mittal, K. G. Orrell, and V. Sik, *J. Chem. Soc., Dalton Trans.*, 1986, 961.
7 D. Seebach, K-H. Greiss, A. K. Beck, B. Graf, and H. Daum, *Chem. Ber.*, 1972, **105**, 3280.
8 E. W. Abel, A. R. Khan, K. Kite, K. G. Orrell, and V. Sik, *J. Chem. Soc., Dalton Trans.*, 1980, 1169.
9 D. A. Kleier and G. Binsch, DNMR3 Program 165, Quantum Chemistry Program Exchange, Indiana University, 1970.
10 G. Binsch and H. Kessler, *Angew. Chem., Int. Ed. Engl.*, 1980, **19**, 411.
11 M. Karplus, *J. Chem. Phys.*, 1959, **30**, 11.
12 C. W. Haigh, *J. Chem. Soc. A*, 1970, 1682.
13 E. W. Abel, P. K. Mittal, K. G. Orrell, V. Sik, and T. S. Cameron, *J. Chem. Soc., Chem. Commun.*, 1984, 1312.

Received 1*st November* 1985; *Paper* 5/1924